George Massey Tunnel Replacement Project

CANADA STARTS HERE | BC JOBS PLAN

BRITISH COLUMBIA | Ministry of Transportation and Infrastructure

Section 16.3

UNDERWATER NOISE MODELLING STUDY

Technical Volume

TABLE OF CONTENTS

LIST OF FIGURES

LIST OF TABLES

1.0 Underwater Noise Modelling

Computational acoustic models were used by JASCO Applied Sciences Ltd. to predict the noise footprints of Tunnel decommissioning and bridge construction activities. The appendix presents the results of this modelling as well as the assumptions made regarding construction scenarios, equipment types, and source noise levels.

1.1 Modelled Construction Noise Scenarios

Acoustic modelling was conducted for six construction scenarios as summarized in **Table 1** to help predict Project-related changes in underwater noise levels within Fraser River South Arm, and Deas and Green Sloughs: impact pile driving; vibratory pile driving; vibrodensification; removal of sediment overlying the Tunnel; lifting one Tunnel segment; and Tunnel decommissioning involving simultaneous sediment removal, rip-rap removal, and lifting of a Tunnel segment. All modelling scenarios considered the influence of bathymetry and riverbed geoacoustics on waterborne sound propagation.

Table 1 Specifications of Modelled Construction Scenarios

Scenario	Description	Noise Source(s)	Source Coordinates
1	Impact hammer driving of a cylindrical pile along the edges of Deas Slough	Impact hammer	49° 6.911' N 123° 4.082' W
2	Vibratory hammer driving of a cylindrical pile along the edges of Deas Slough	Vibratory hammer	49° 6.911' N 123° 4.082' W
3	Vibrodensification in Deas Slough	Vibrodensifier	49° 6.911' N 123° 4.082' W
4	Cutter suction dredging at Tunnel crossing	Cutter suction dredge	49° 7.292' N 123° 4.562' W
		Tug 1 (downstream)	49° 7.318' N 123° 4.598' W
5	Tug and barge activity during crane lift of Tunnel segments	Tug 1 (downstream)	49° 7.3179' N 123° 4.598' W
		Tug 2 (upstream)	49° 7.318' N 123° 4.430' W

Scenario	Description	Noise Source(s)	Source Coordinates
6	Simultaneous removal of sediment and rip-rap and crane lift of Tunnel segments	Cutter suction dredge	49° 7.314' N 123° 4.581' W
		Clamshell dredge	49° 7.306' N 123° 4.459' W
		Tug 1	49° 7.329' N 123° 4.601' W
		Tug 2	49° 7.298' N 123° 4.561' W
		Tug 3	49° 7.244' N 123° 4.513' W
		Tug 4	49° 7.226' N 123° 4.492' W
		Tug 5	49° 7.212' N 123° 4.467' W
		Tug 6	49° 7.195' N 123° 4.447' W
		Tug 7	49° 7.240' N 123° 4.355' W
		Tug 8	49° 7.259' N 123° 4.379' W
		Tug 9	49° 7.274' N 123° 4.340' W
		Tug 10	49° 7.292' N 123° 4.422' W
		Tug 11	49° 7.290' N 123° 4.439' W
		Tug 12	49° 7.320 N 123° 4.479' W

1.1.1 Construction Activities Excluded from the Model

The modelling focused on construction activities expected to generate underwater sound levels that would exceed the existing background ambient noise. Activities such as separation of the bulkhead connections between Tunnel segments may require the use of specialized equipment. Potential effects of underwater noise generated by such equipment will be assessed using sound data collected during Tunnel decommissioning and mitigation measures will be put in place to manage such effects as appropriate.

1.2 Source Noise Levels for Construction Activities

1.2.1 Impact and Vibratory Driving of Cylindrical Piles

Underwater acoustic sound generated from impact and vibratory driving at the pile wall was predicted using JASCO's pile driving source model (MacGillivray 2013). The forcing function (the applied force from the hammer versus time) at the top of the pile is related to the proposed hammer type and hammer energy. The forcing function was modelled with the GRLWEAP 2010 model (Pile Dynamics Inc. 2010), which includes a large database of various hammers and associated manufacturers' specifications.

The predicted forcing function was coupled to a one-dimensional finite-difference model to account for the vibrational coupling between the pile and the surrounding water and sediments. The pressure radiating from the pile wall was computed using a vertical array of individual sources (monopoles) distributed along the pile to account for the boundary condition between the pile wall and surrounding water. A typical impact hammer for the two-metre diameter steel pipe piles was selected based on a review of existing hammers and on a discussion with the Project engineers. The impact hammer type that was modelled (a Delmag D100-13 with a rated energy output of 360 kJ) was chosen based on communication with the Project engineers and a review of existing hammer types used in North America for the proposed pile diameter, length, and pile materials. Based on the manufacturer's specifications, the impact hammer was assumed to operate at 35 blows per minute at the maximum hammer energy (Hammer & Steel 2014). The vibratory hammer type that was modelled was an APE-400B with a rated power output of 738 kJ. **Table 2** shows the pile dimensions and hammer specifications that were used in the GRLWEAP and JASCO pile driving models to compute source levels for both impact and vibratory pile driving.

Table 2 Engineering Specifications of Pile Driving Equipment

Hammer Method	Pile Size (diameter x length)	Hammer Type	Hammer-Energy (kJ)	RAM Mass (tons)	Blows Per Minute
Impact	2 m x 85 m	Delmag-D100-13	360	10.01	35
Vibratory	2 m x 85 m	APE-400B	738	0.35	-

Sound levels were computed for distances of up to 100 m from the source (i.e., far-field source levels) by propagating the pressure field of each individual monopole source from the pile driving source model out to 100 m range using JASCO's Full-Waveform Range-dependent Acoustic Model (FWRAM; see **Section 1.3.1**). The 1/3-octave band received levels were then back-propagated to the standard one-metre reference range using transmission loss that was computed with JASCO's Marine Operations Noise Model (MONM; see **Section 1.3.2**). Sound levels from the pile-driving scenarios described in **Table 1** were then modelled with MONM using the far-field source levels.

The 1/3-octave band far-field source levels for the impact hammer are shown in **Figure 10**. The broadband source level for this activity is 220 dB re 1 μPa^{2}s at 1 m. The forcing function modelled with GRLWEAP for this hammer, and the monopole source spectra for impact pile driving sampled at three different depths, are shown in **Figure 11** and **Figure 12** respectively.

The 1/3-octave source levels for the vibratory hammer are shown in **Figure 13**. The estimated broadband source level for this activity is 217 dB re 1 μPa at 1 m. The forcing function with GRLWEAP for this hammer is shown in **Figure 14**. The monopole source spectra for vibratory pile driving sampled at three different depths are shown in **Figure 15**.

1.2.2 Vibrodensification

Source levels for vibrodensification were obtained from measurements taken by JASCO at the Roberts Bank Terminals, B.C. (Austin 2007). The maximum of the two measurements in each 1/3-octave band between 10 Hz and 40 kHz were used. Source levels above 40 kHz were extrapolated using the trend between 20 and 40 kHz. The broadband source level for the vibrodensifier used in this modelling study was 182 dB re μPa at 1 m. The modelled 1/3-octave band source levels are shown in **Figure 13**. The modelled source depth for vibrodensification was taken to be at mid-water column (2.5 m).

1.2.3 Sediment Removal to Facilitate Tunnel Decommissioning

Source levels for cutter suction dredging operations to remove sediment overlying the Tunnel were derived from measurements of a cutter suction dredge obtained by JASCO for the Deltaport Third Berth project (Zykov et al. 2007). Source levels were extrapolated above the maximum measured frequency of 40 kHz using the trend between 20 and 40 kHz. Sounds below 1 kHz were assumed to originate from inside the dredge hull, whereas sounds above 1 kHz were assumed to originate from the cutter head at the riverbed (Robinson et al. 2011). The source depth for the dredge hull was modelled at 2.14 m below the water surface; the source depth of the cutter head was modelled at one metre above the riverbed. The modelled broadband source level of the cutter suction dredge was 182 dB re 1 µPa and **Figure 13** shows the modelled 1/3-octave band source levels.

Source levels for clamshell dredging associated with Tunnel decommissioning were based on published measurements of two dredges (Miles et al. 1987, Dickerson et al. 2001). Where measurements were presented as received levels at a specified distance rather than source levels at a reference of one metre, source levels were back-propagated using environment-based transmission loss modelling. Averaged 1/3-octave band source levels were then selected for the dredge. The source depth for the clamshell dredge was set to half the local water depth since losses due to bottom and surface interactions will be less for a source at mid-depth than for a source near the seafloor or surface. The modelled broadband source level of the clamshell dredge was 176 dB re 1 µPa. **Figure 13** shows modelled 1/3-octave band source levels.

1.2.4 Tug and Barge Operations

Tugs and barges will be used to support cranes and dredging operations during Project construction. The river tug *Seaspan Venture* was identified as a representative barge-towing vessel, based on a discussion with the Project engineers and a review of similar vessels currently operating in the Fraser River. Source levels for the river tug were estimated from measurements, performed by JASCO, of a harbour tug transiting at 7.5 kts near Roberts Bank terminals (Warner et al. 2013). Source levels for the river tug were reduced by 5.7 dB to account for the difference in total engine power between it and the larger, measured harbour tug (**Table 3**). **Figure 13** shows the modelled 1/3-octave band source levels for river tugs. The broadband source level was 166 dB re 1 µPa at one metre. Source levels were extrapolated below 20 Hz using a constant value equal to the 20 Hz 1/3-octave band level.

Table 3 Tugboat Specifications

Type	Length	Width	Draught	Source depth	Total engine power (kW)
Harbour tug	30 m	13 m	3.17 m	1.47 m	4.476
River tug	19.5 m	7 m	3.17 m	1.47 m	1.268

It was assumed that all construction barges will be towed by tugs. Barges might, however, have vibrating machinery onboard that could conduct a small amount of underwater sound into the river through the barge's hull. When sound from tug and barge operations was modelled, it was assumed that the barge contribution was not substantial compared to sound generated by the tugs' propulsion systems.

1.3 Sound Propagation Model

1.3.1 Full-Waveform Range-Dependent Acoustic Model

JASCO's Full-Waveform Range-dependent Acoustic Model (FWRAM) was used to simulate pulse propagation to produce synthetic waveform traces of the impact pile driving pulses. These calculations were used to determine the rms and peak pulse pressure as a function of range from the source, and consequently the range-dependent conversion factor between SEL and rms SPL.

FWRAM computes synthetic pressure waveforms at receiver locations on a range-depth grid using Fourier synthesis to generate full-waveform sound field predictions in finely spaced frequency bands at the individual frequencies. Environmental inputs for FWRAM include bathymetry, water sound speed profiles, and physical properties of the riverbed (geoacoustic profiles).

1.3.2 Marine Operations Noise Model

Sound levels were modelled using MONM, which predicts underwater sound propagation in range-varying acoustic environments. MONM computes acoustic fields in three dimensions by modelling transmission loss (TL) along evenly spaced two-dimensional (2-D) radial traverses covering a 360° swath from the source, an approach commonly referred to as $N \times$ 2-D. The model fully accounts for depth and range dependence of several environmental parameters, including bathymetry and sound speed profiles for the water column and the sub-bottom sediments. It also accounts for the additional reflection loss at the riverbed that is due to partial conversion of incident compressional waves to shear waves at the riverbed and sub-bottom interfaces through a complex density approximation (Zhang and Tindle 1995).

The acoustic environment is sampled at a fixed-range step along radial traverses. MONM treats frequency dependence by computing acoustic TL at the centre frequencies of 1/3-octave bands. Broadband received levels are summed over the received 1/3-octave band levels, which are computed by subtracting band TL values from the corresponding source levels. MONM's predictions have been validated against experimental data from several underwater acoustic measurement programs (Aerts et al. 2008, Funk et al. 2008, Ireland et al. 2009, O'Neill et al. 2010, Warner et al. 2010, Hannay et al. 2013). For this study, MONM was used to compute TL for 1/3-octave bands centred between 10 Hz and 5 kHz. To model non-pulsed sources such as vibrodensification, tugs, dredgers, and vibratory pile drivers, MONM was used to predict the SPLs on the $N \times$ 2-D grid. For impact pile driving, MONM was used to model the single-strike SELs.

The transmission loss computed by MONM was further corrected to account for the attenuation of acoustic energy by molecular absorption in water. The volumetric sound absorption is quantified by an attenuation coefficient, expressed in units of decibels per kilometre (dB/km). The absorption coefficient depends mainly on the sound frequency, but also on the temperature, salinity, and hydrostatic pressure of the water. In general, the absorption coefficient increases with the square of frequency. The absorption of acoustic wave energy has a noticeable effect (>0.05 dB/km) at frequencies above 1 kHz. At 10 kHz, the absorption loss over 10 km can exceed 10 dB.

Transmission loss was approximated for bands between 6.3 and 50 kHz by using the TL computed at 5 kHz and applying the correct frequency-dependent absorption coefficient in each band. In this study, the absorption coefficients were calculated based on water temperature at 10°C and salinity of 0.5 parts per thousand and a water depth of 2.5 m.

Sound levels were modelled at eight different receiver depths from 2.5 m to the riverbed, distributed vertically in the water column. Modelled received levels were gridded separately in each horizontal plane (i.e., at each modelled receiver depth). To generate a conservative estimate, the modelled results were obtained by collapsing the stack of grids into a single plane using a maximum-over-depth rule, which means that the sound levels at each planar point are taken to be the maximum value from all modelled depths in the water column for that point.

1.3.3 Calculation of Peak SPL, rms SPL, and SEL for Impact Pile Driving

For pulsed sound sources, MONM computes per-pulse SEL in 1/3-octave bands, but does not directly predict the 90 per cent rms SPL or peak SPL. Although the 90 per cent rms SPL and peak SPL are easily measured in situ, these metrics are generally more difficult to model than per-pulse SELs. In addition, the adaptive integration period to model rms SPLs, implicit in the definition of the 90 per cent rms SPL, is highly sensitive to the specific multipath arrival pattern from an acoustic source and can vary greatly with distance from the source or with receiver depth. Nonetheless, per-pulse SEL and SPL are related, and SEL can therefore be used to estimate SPL.

In this study, FWRAM was used to calculate peak SPL and rms SPLs for impact pile driving. The pressure field from the pile driving source model was modelled at frequencies from 10 Hz to 2 kHz in 0.5 Hz steps to generate synthetic pressure waveforms along a single transect. These waveforms were then analyzed to determine peak SPL and rms SPL as a function of range from the source. The representative transect, which extended 1.2 km from the source, heading 268 degrees west, was chosen for its uniform bathymetry.

The FWRAM pulse length and waveform predictions were used to derive a range-dependent conversion function between SEL and rms/peak SPL. The resulting conversion functions were applied to the per-pulse SEL predictions from MONM to compute the rms SPLs and peak SPLs. The conversion functions for per-pulse SEL to rms SPL and peak SPL are shown in **Figure 16** as a function of source-receiver offset.

Long-term exposures to high-intensity anthropogenic noise can temporarily or permanently reduce an animal's hearing sensitivity. Cumulative sound exposure is generally measured as the total sound energy an organism receives over some period. The cumulative SEL for impact pile driving was computed for sequences of pile driving blows that could occur over 24 hours. The number of strikes required to drive each pile is not known, so three durations of pile driving activity were modelled over a 24-hour period for each scenario (see **Table 1**): one minute, 10 minutes, and 100 minutes.

1.3.4 Calculation of Sound Level Contours

The predicted received SPLs and SELs were contoured to show the estimated acoustic footprint for each scenario. Sound level contours were converted to GIS layers, visible on maps of the study area. For each duration scenario, the 95th percentile radius ($R_{95\%}$) and the maximum radius (R_{max}) for each sound threshold level were tabulated.

1.4 Environmental Parameters

1.4.1 Bathymetry

High-resolution bathymetry data within several kilometres of the Tunnel, collected as part of the river hydraulics and river morphology study for the Project, were used to develop a bathymetry model for the study area. Water depths in the Fraser River vary depending on tidal cycle and time of year. High-water conditions are most conservative with respect to the distance that sound propagates in the water because sound energy is more rapidly absorbed by bottom sediments in shallow water. Therefore, the data were adjusted to a high-water datum of 2.0 m to accommodate high-water stands during the fall and winter months. Maximum water depths in the study area are less than 30 m. Bathymetry data were re-projected onto a 10 m x 10 m grid in UTM zone 10 N for use with MONM.

1.4.2 Water Depth

Water depths in the river vary depending on the tides and the time of year (seasonal variations). High-water conditions are most conservative with respect to the distance that sound propagates in the water. Therefore, the data were adjusted to a high-water level of 2.0 m to accommodate high-water stands during the fall and winter.

A water depth of five metres, which corresponds to a high high tide, was assumed for modelling pile driving along the edge of Deas Slough. Much of the actual Project-related construction along the edge of Deas Slough would occur under lower water conditions or in the dry with low tide. Effectiveness of construction pads with granular fills as a way to mitigate underwater noise was investigated, subsequent to completion of modelling. Propagation through the granular fill and the underlying soils is expected to attenuate sound levels generated by pile driving and reduce underwater noise emissions. Given these considerations, levels of underwater noise emissions generated by the actual construction are expected to be somewhat lower than the results of the modelling presented in this document.

1.4.3 Geoacoustic Properties

Sound propagation is influenced by the physical properties of the river bottom sediments, including the density, compressional wave (P-wave) speed, shear wave (S-wave) speed, compressional wave attenuation, and shear wave attenuation of the riverbed sediments. The main riverbed sediment types in the study area are water-saturated silts and silty sands, based on borehole and penetration data (Puar 1996). The geoacoustic properties for these types of sediments (**Table 4**) were estimated on empirical formulas presented by Hamilton (1980).

Table 4 Geoacoustic Parameters used for Modelling the Riverbed Sediments

Depth below seafloor (m)	Sediment type	Density (g/cm^3)	P-wave speed (m/s)	P-wave attenuation (dB/λ)	S-wave speed (m/s)	S-wave attenuation (dB/λ)
0–3	Clayey silt	1.5 – 1.4	1537 – 1523	0.18	180	2.0
3–29	Silty sand	1.4 – 1.6	1523 – 1529	0.18 – 0.20		
>29	Sandy silt	1.6	1529	0.20		

1.4.4 Sound Speed Profile

The sound speed profile in the water column was derived using the empirical Marczak equation (Marczak 1997) or fresh water. The estimated sound speed in water at the study location is approximately 1,457 m/s based on the average water temperature of 10°C from late summer to early spring. Average seasonal water temperature values were obtained from the DFO Fraser River Environmental Watch Report (DFO 2013).

2.0 Noise Source Modelling Results

It was assumed that impact pile driving would operate at 35 blows per minute, totalling one minute (35 blows), 10 minutes (350 blows), and 100 minutes (3,500 blows) during a 24-hour period. Under that assumption, 15.4 dB, 25.4 dB, and 35.4 dB were added to the single-pulse SEL to yield 24-hour SEL results. **Table 5** presents the 95th percentile contour radii of 24-hr (one-, 10-, and 100-minute piling) SEL unweighted and M-weighted (pinnipeds) contours for impact pile-driving (scenario 1). Corresponding contour maps of unweighted and M-weighted SEL are provided in **Figure 1** through **Figure 3**. The M-weighting curves reduce sound at low and high frequencies; however, the pinniped M-weighting curve is nearly flat over the frequency range generated by the impact hammer. In **Table 5** and **Table 6**, $R_{95\%}$ is the radius of a circle centred at the source that encompasses 95 per cent of the area ensonified to the threshold value; R_{max} is the maximum distance from the source to the given noise threshold in any direction.

Table 5 Radii (95%), of 24-hr (1-, 10-, and 100-minute Piling) Unweighted SEL and M-weighted SEL Contours for Impact Pile Driving (Scenario 1)

SEL (dB re 1 µPa²•s)	1 min	10 min	100 min
FHWG threshold fish < 2 g (183 dB)[1]	91	286	698
FHWG threshold fish ≥ 2 g (187 dB)[1]	69	169	602
Southall M-weighted pinniped threshold (186 dB)[2]	66	180	618

Notes: radii measured in metres
[1]Source: (FHWG 2008)
[2]Source: (Southall et al. 2007)

The broadband (10 Hz to 50 kHz) rms SPL radii for the NMFS injury threshold (190 dB re 1 µPa) was computed with 53 m, based on the estimated offset curves described in **Section 1.3.3**. The corresponding contour map of rms SPL is provided in **Figure 4**, including the contours for the ZAA for the 50th (L_{50}) and 95th (L_{95}) exceedance percentiles. **Table 6** presents the peak SPL radii to injury thresholds for scenario 1. The 95th percentile radius for the ZAA extends to 7,460 m for both L_{50} and L_{95}.

Table 6 Radii (Rmax) of Peak SPL Injury Thresholds for Impact Pile Driving (Scenario 1)

Acoustic Injury Criteria	Peak SPL (dB re 1 µPa)
FHWG Fish < 2 g (206 dB) [1]	53
B.C. MPDCA Threshold Fish (210 dB) [1]	42
Southall M-weighted Pinniped Threshold (218 dB) [2]	27

Notes: radii measured in metres
[1]Source: (FHWG 2008)
[2]Source: (Southall et al. 2007)

Table 7 presents 95th percentile and maximum contour radii for vibratory pile driving (scenario 2), vibrodensification (scenario 3), cutter suction dredging (scenario 4), tug and barge activity during crane lift of Tunnel segments (scenario 5), and simultaneous dredging at Tunnel crossing and crane lift of Tunnel segments (scenario 6). Corresponding contour maps for unweighted maximum-over-depth broadband (10 Hz to 50 kHz) rms SPLs in dB re 1 µPa are shown in **Figure 5** to **Figure 9**. The grey and black contours indicate the ZAA for L_{50} and L_{95}. The 95th percentile radii at 120 dB re 1 µPa rms SPL are 951 m in Deas Slough, and 2,746 m in the Fraser River South Arm. The maximum radii for the ZAA extend to 5,500 m and 6,250 m for L_{50} and L_{95}, respectively (**Table 8**).

Table 7 Radii (95%) of Unweighted rms SPL Contours for Scenarios 1 through 6 (All Distances in Metres)

rms SPL (dB re 1 µPa)	Scenarios					
	1	2	3	4	5	6
120	3043	593	951	2726	441	3447
130	2956	346	319	980	79	1275
140	2939	228	52	230	27	357
150	2742	88	21	52	<10	52
160	1233	58	<10	11	n/a	10
170	741	37	n/a	<10	n/a	<10
180	104	22	n/a	n/a	n/a	n/a
190	53	9	n/a	n/a	n/a	n/a
200	30	<5	n/a	n/a	n/a	n/a

Note: n/a = indicates levels were not reached.

Table 8 Radii (Rmax) of Unweighted SPL Contours for the Zone above Ambient Levels for Scenarios 1 through 6 (All Distances in Metres)

rms SPL (dB re 1 µPa)	Scenarios					
	1	2	3	4	5	6
ZAA (L_{50})	7,460	5,503	3,540	5,512	5,299	5,502
ZAA (L_{95})	7,460	6,256	3,545	5,515	5,548	5,565

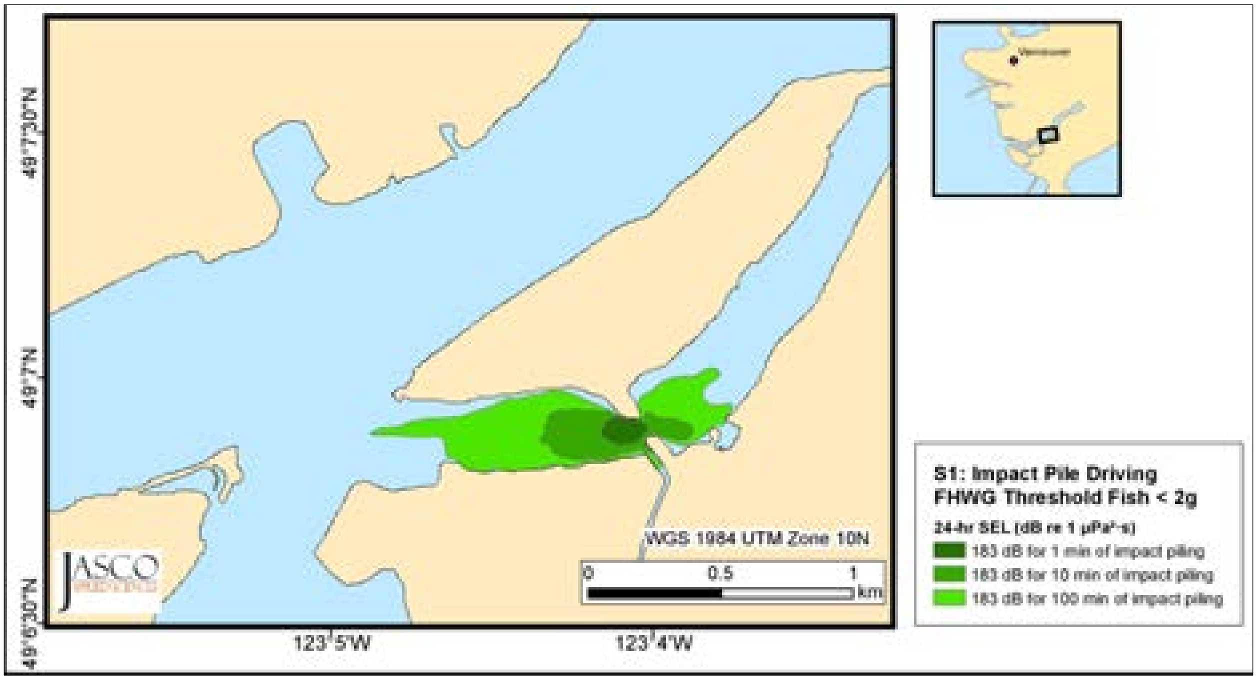

Figure 1 **Contour Map of FHWG SEL Threshold for Fish Weighing Under Two Grams for 1, 10, and 100 Minutes of Impact Piling at Deas Slough.**

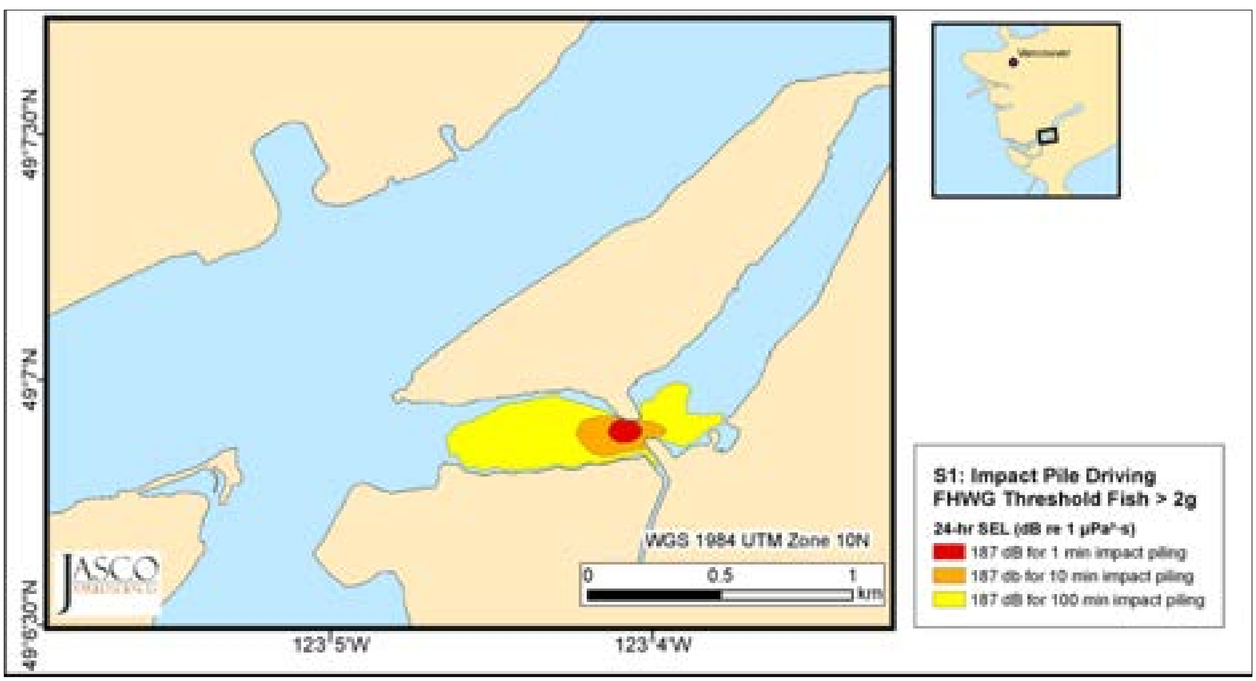

Figure 2 **Contour Map of FHWG SEL Threshold for Fish Weighing Over Two Grams for 1, 10, and 100 Minutes of Impact Piling at Deas Slough.**

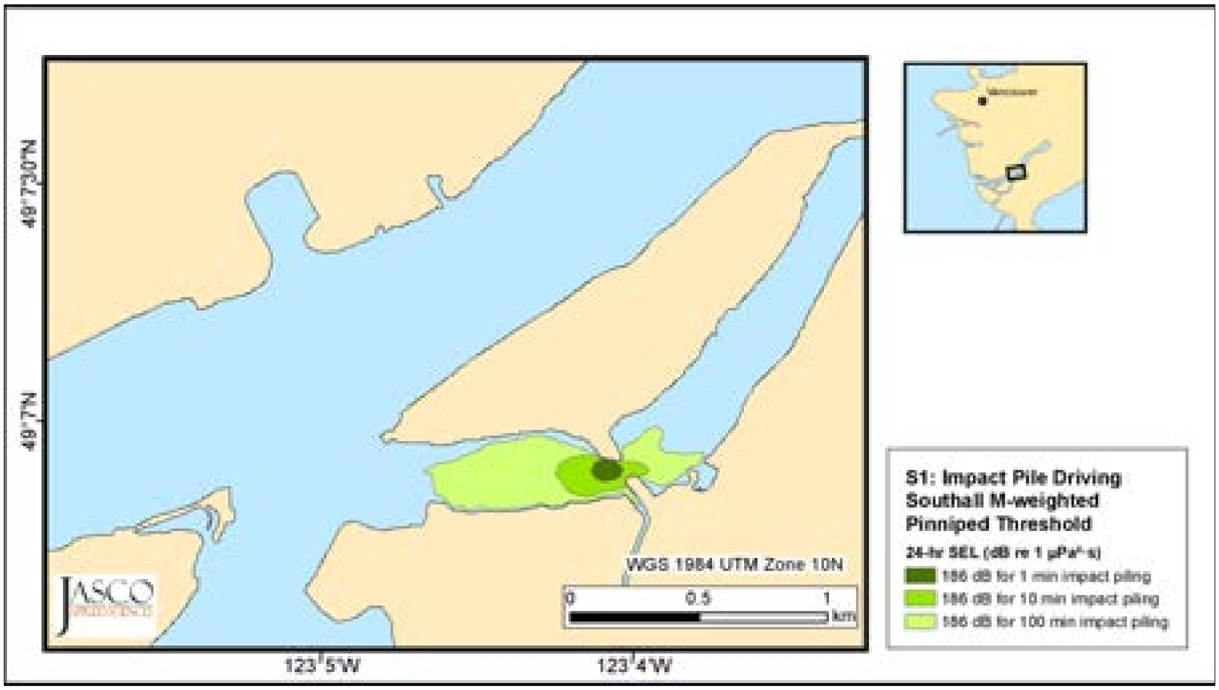

Figure 3 **Contour Map of Southall et al. (2007) Pinniped M-weighted SEL Threshold for 1, 10, and 100 Minutes of Impact Piling at Deas Slough.**

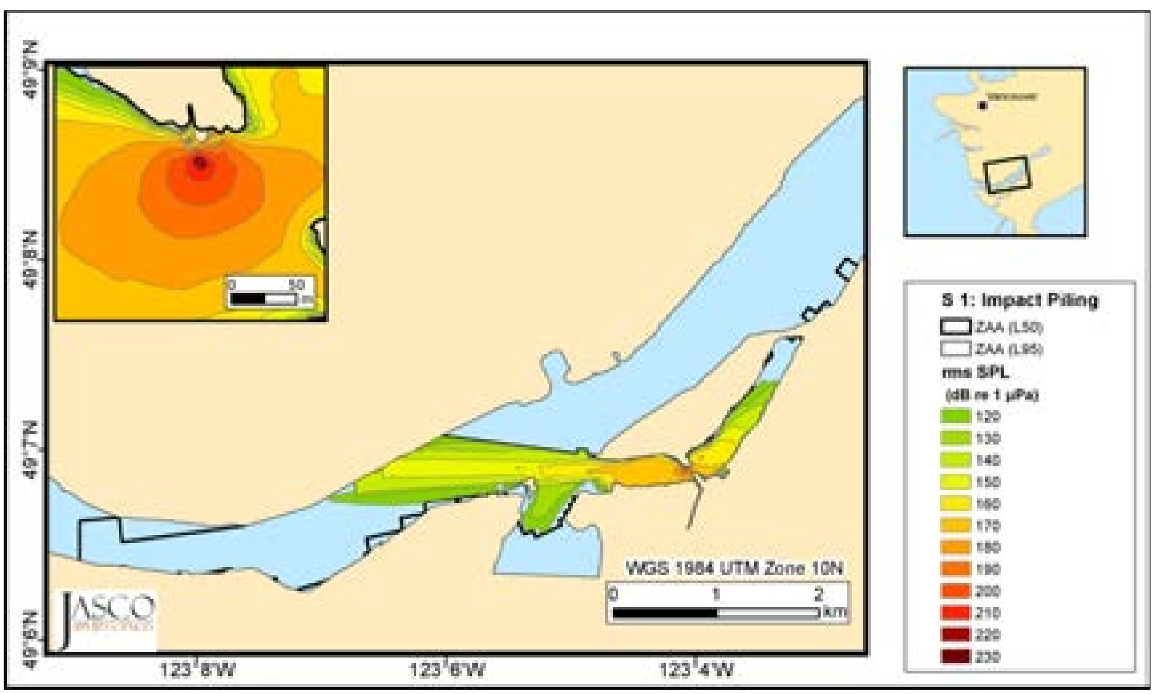

Figure 4 **Broadband Contour Map of rms SPL for Impact Piling at Deas Slough (Scenario 1).**

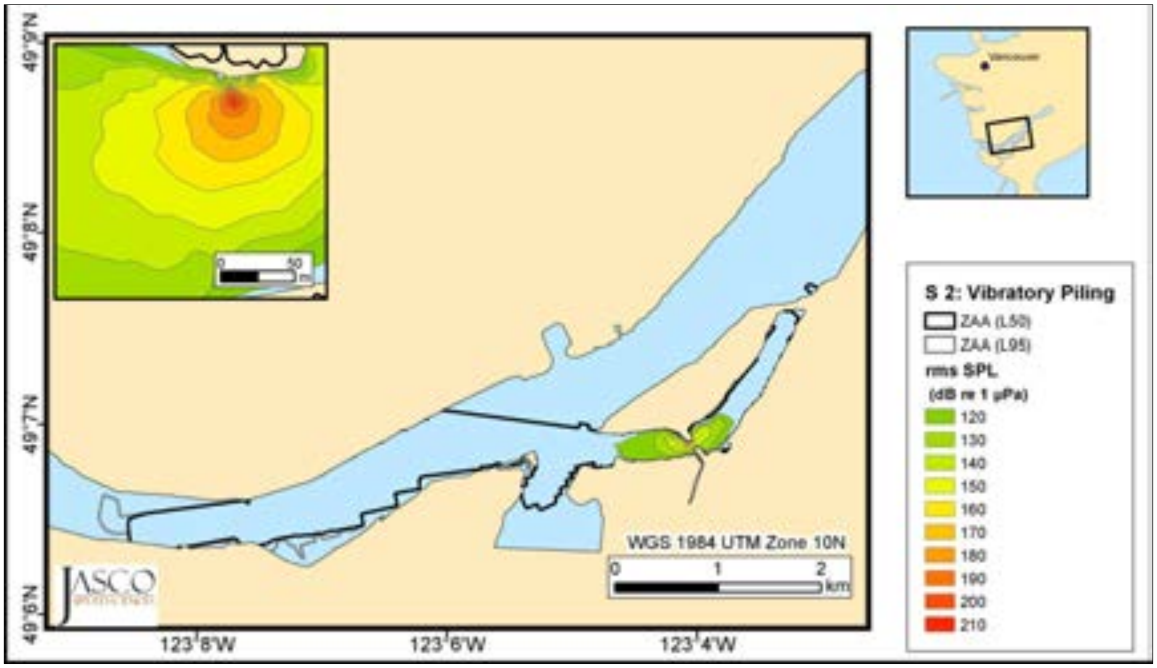

Figure 5 **Broadband Contour Map of rms SPL for Vibratory Piling at Deas Slough (Scenario 2).**

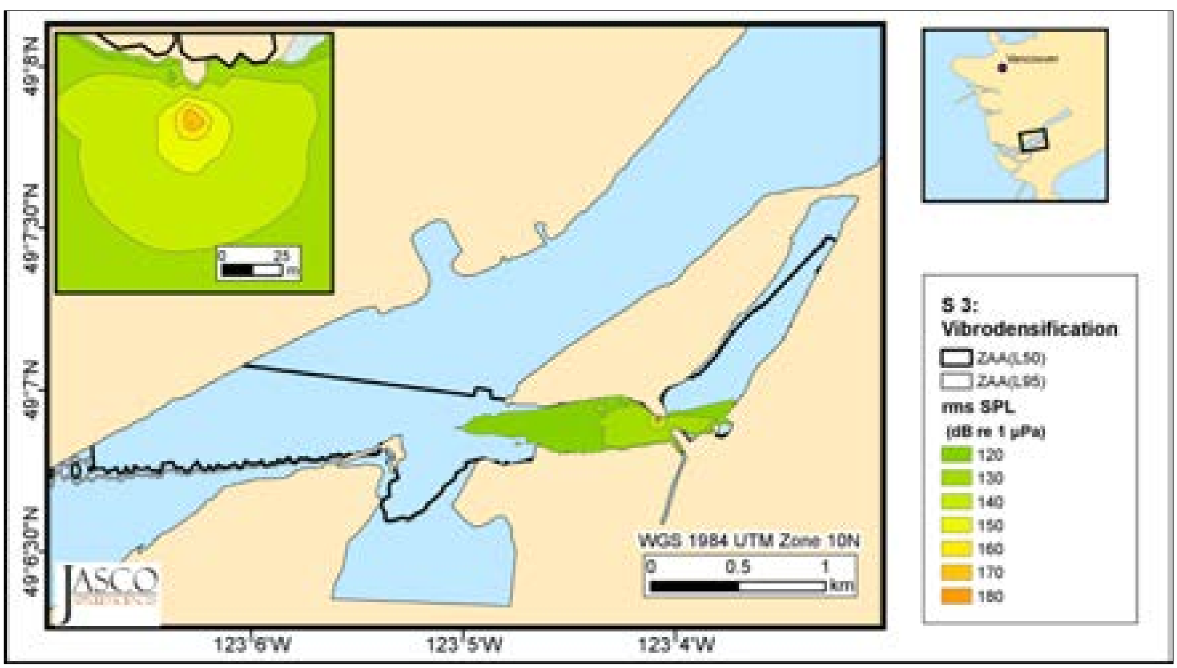

Figure 6 **Broadband Contour Map of rms SPL for Vibrodensification (Scenario 3).**

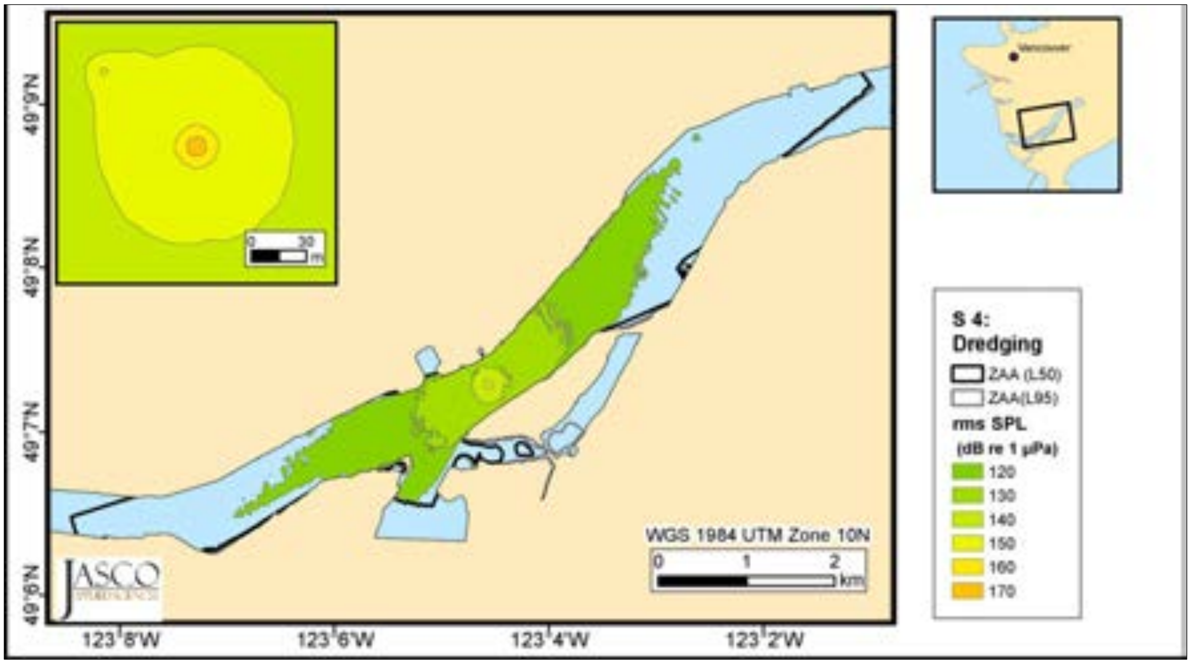

Figure 7 **Broadband Contour Map for Unweighted rms SPL for Cutter Suction Dredge Operations (Scenario 4).**

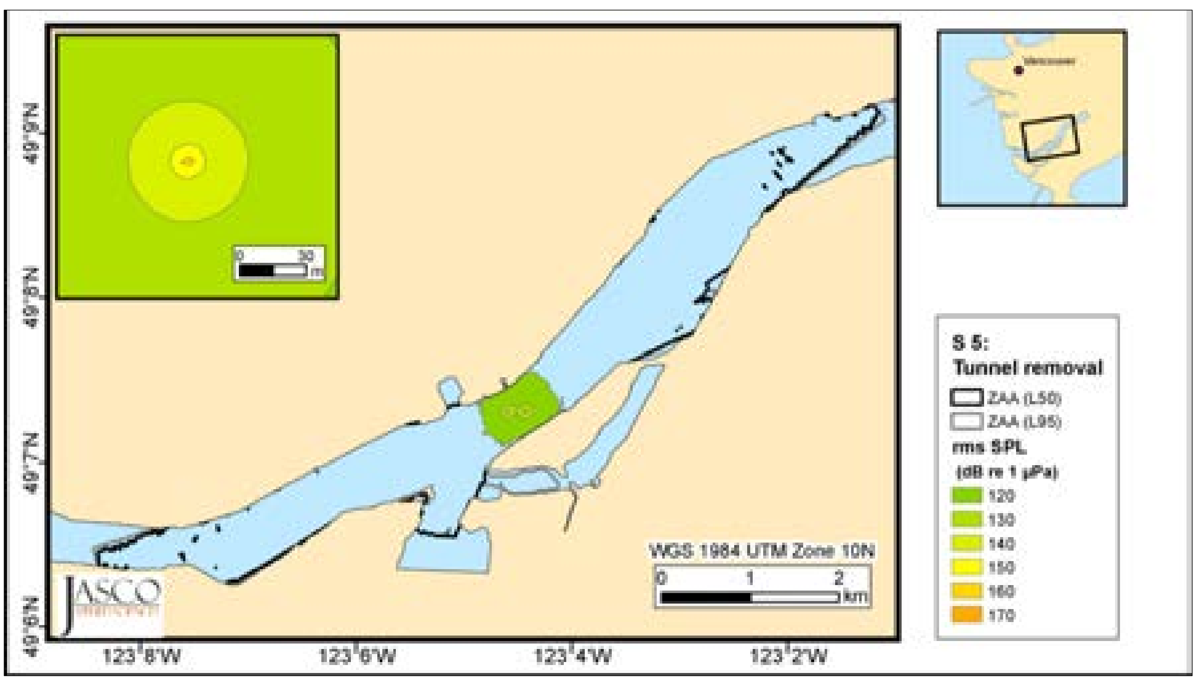

Figure 8 **Broadband Contour Map of rms SPL for Tug and Barge Activities During Crane Lift of Tunnel Segments (Scenario 5).**

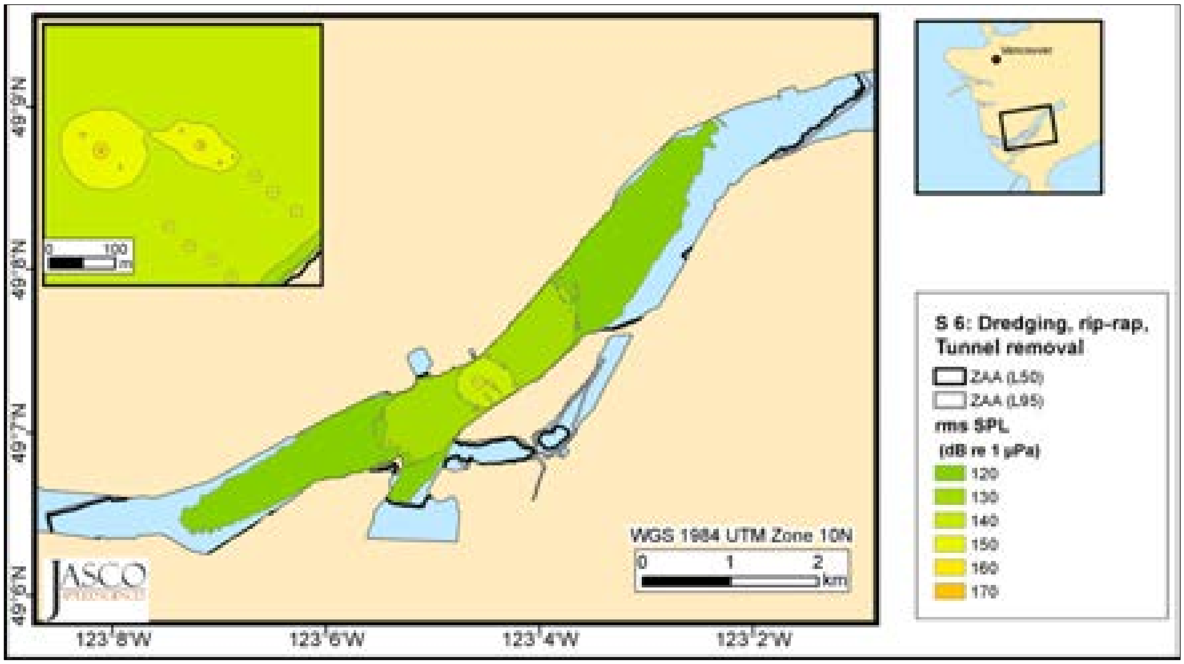

Figure 9 **Broadband Contour Map of rms SPL for Simultaneous Crane Lifting and Dredging Activities (Scenario 6).**

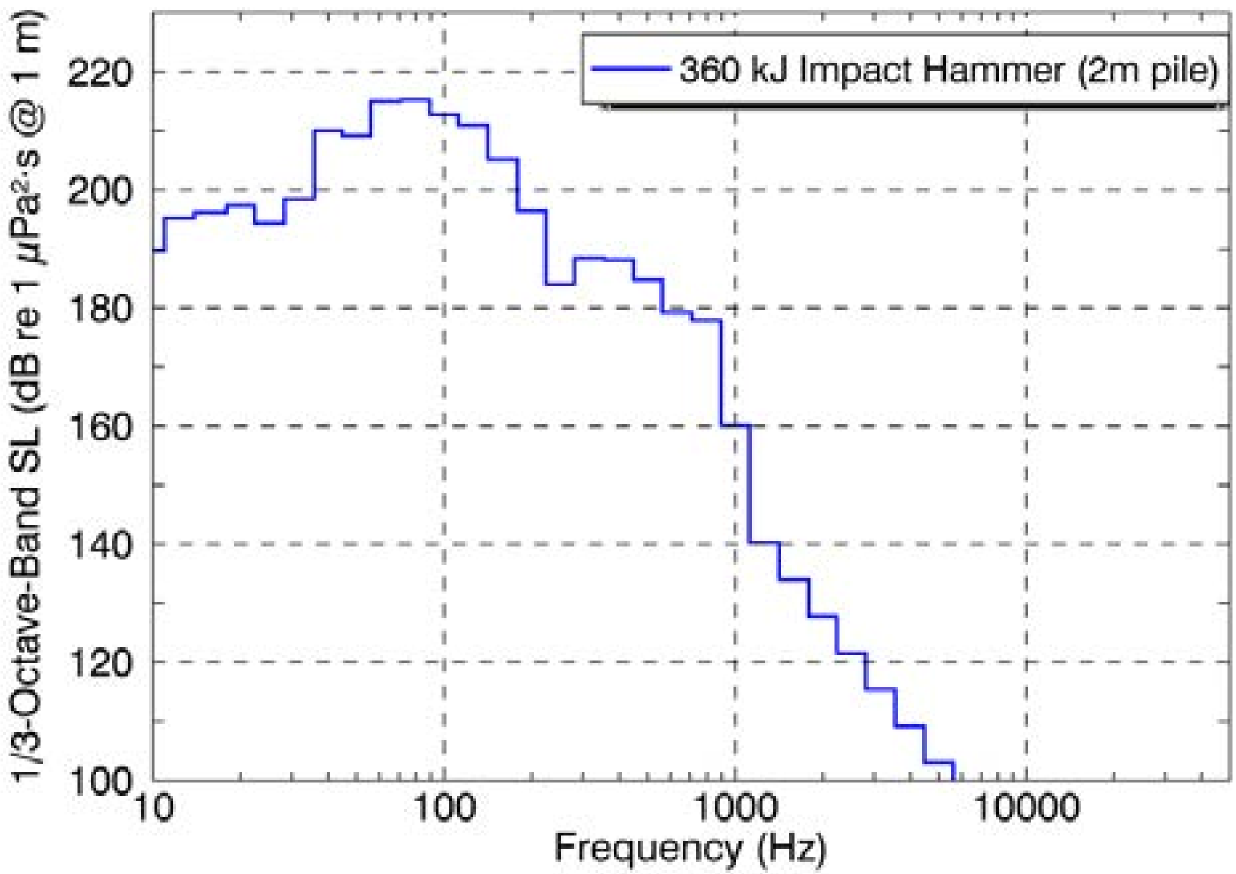

Figure 10 **Modelled 1/3-octave Band Source Levels for Impact Pile Driving.**

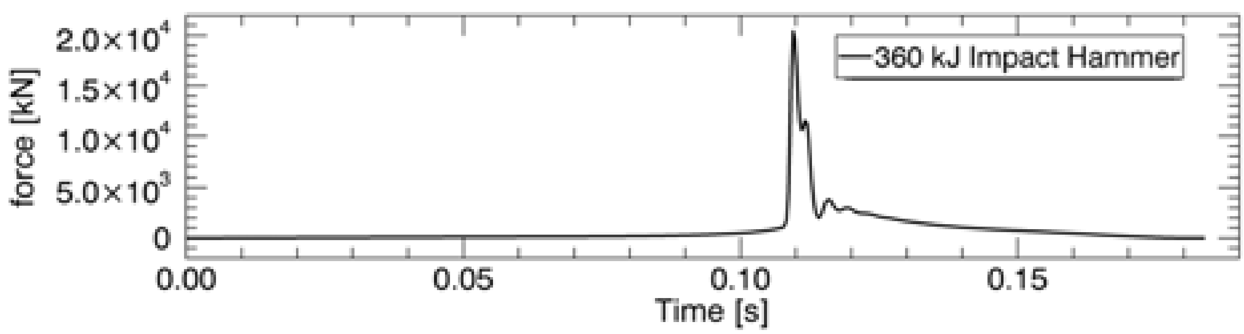

Figure 11 **Modelled Forcing Function at the Top of the 2 m x 85 m Pile, Generated by Delmag D100-13 Impact Hammer.**

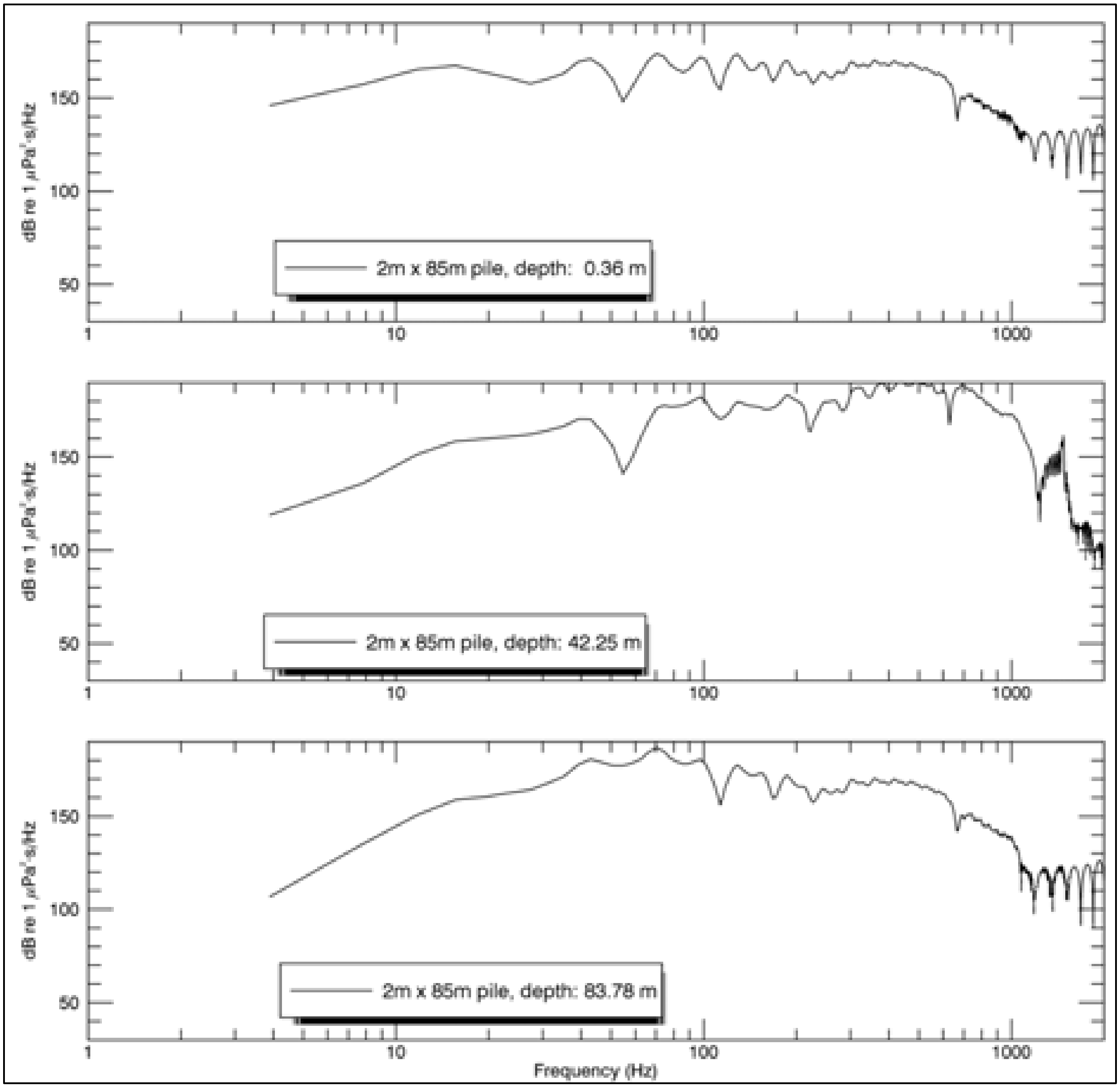

Figure 12 **Modelled Monopole Source Spectra, Sampled at Three Depths Along the Pile, for Impact Hammering of the 2 m x 85 m Pile.**

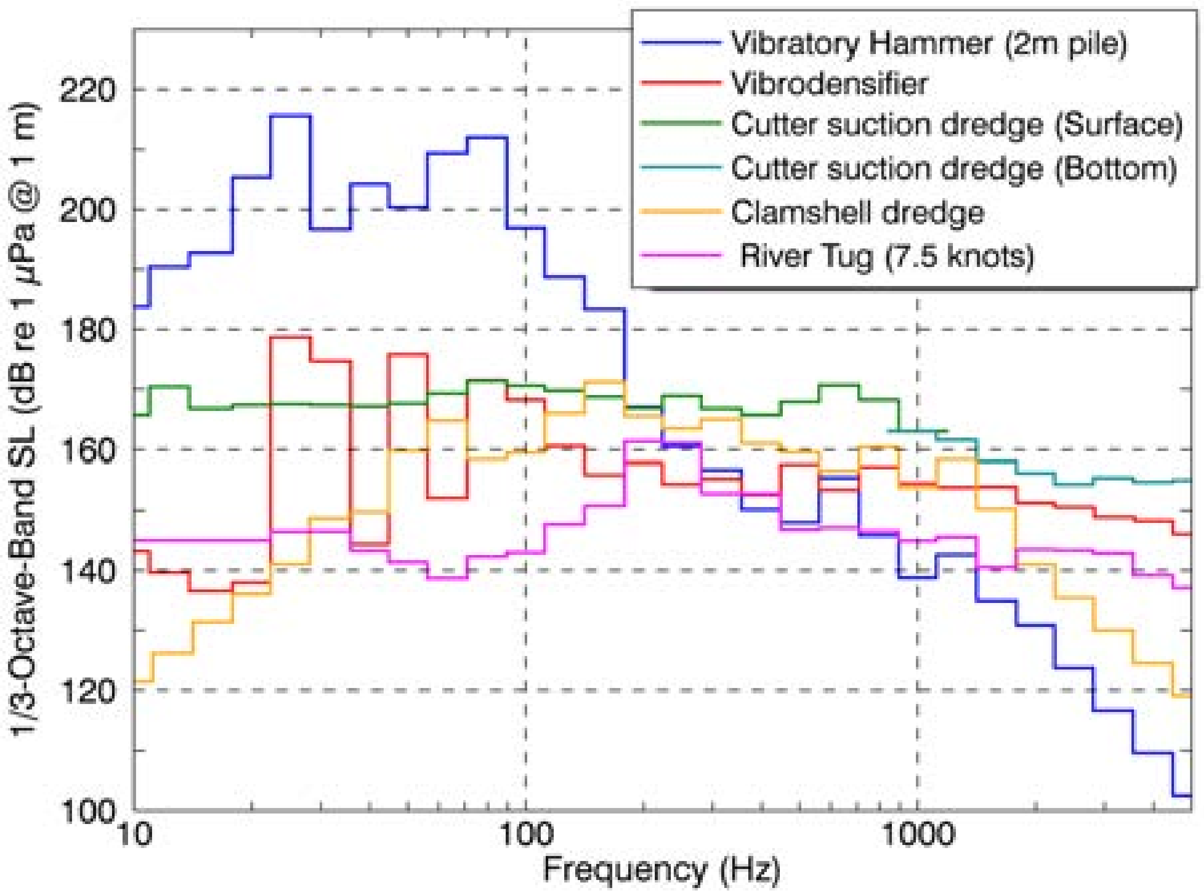

Figure 13 **Modelled 1/3-octave Band Source Levels for Non-pulsed Noise Sources.**

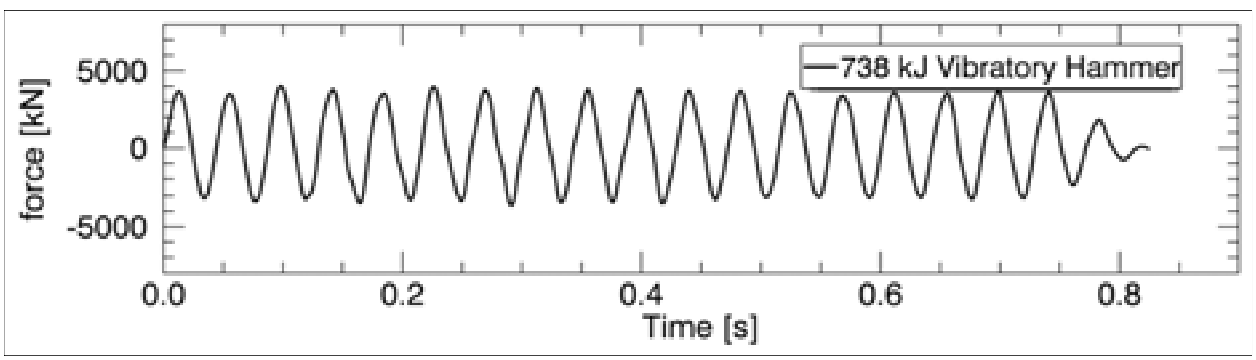

Figure 14 **Modelled Forcing Function at the Top of the 2 m x 85 m Pile, Generated by APE-400B Vibratory Hammer.**

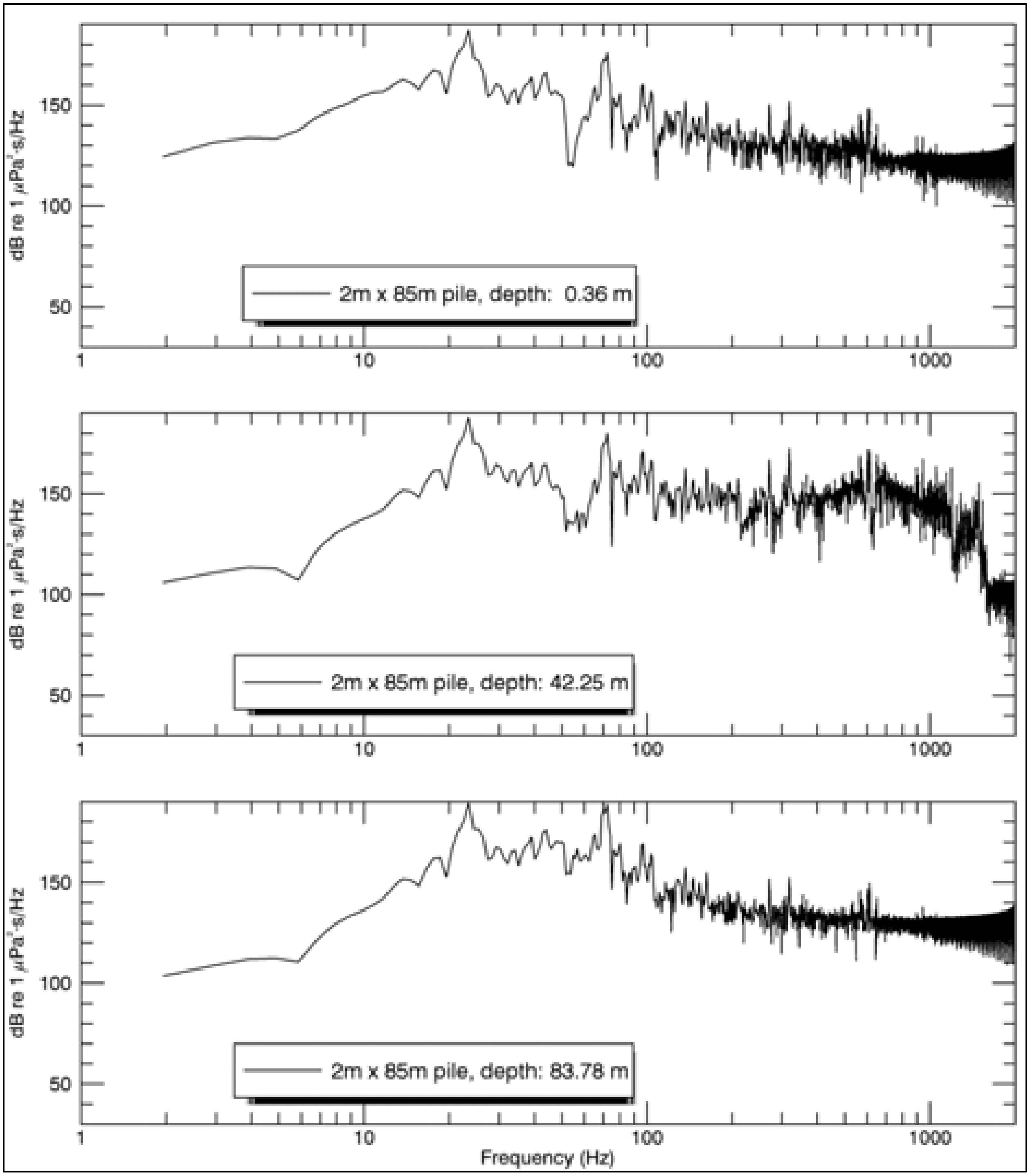

Figure 15 **Modelled Monopole Signature Spectra, Sampled at Three Depths along the Pile, for Vibratory Hammering of the 2 m x 85 m Pile.**

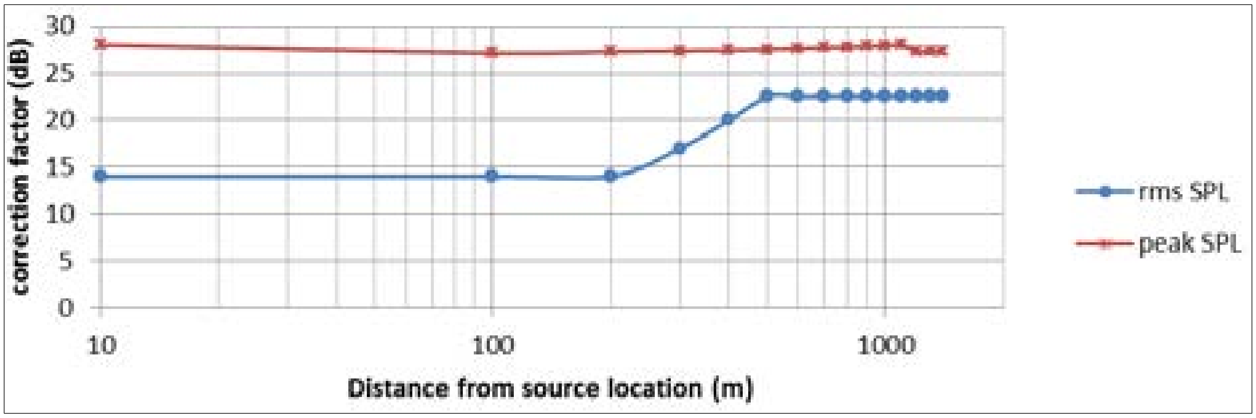

Figure 16 Per-pulse SEL to rms SPL and Peak SPL Conversion Function Versus Distance from Source (m).

3.0 References

Aerts, L., M. Blees, S. Blackwell, C. Greene, K. Kim, D. Hannay, and M. Austin. 2008. Marine mammal monitoring and mitigation during BP Liberty OBC seismic survey in Foggy Island Bay, Beaufort Sea, July-August 2008: 90-day report. LGL Report P1011-1, Prepared by LGL Alaska Research Associates Inc., LGL Ltd., Greeneridge Sciences Inc., and JASCO Applied Sciences for BP Exploration Alaska. Available at http://www.nmfs.noaa.gov/pr/pdfs/permits/bp_liberty_monitoring.pdf.

Austin, M. 2007. Vibro-densification source level study and killer whale acoustics impact report. Jacques Whitford AXYS and JASCO Research Ltd., editors. Appendix F: Marine mammal monitoring program reports. Technical Report, Prepared by JASCO Research Ltd. for Vancouver Port Authority, Victoria, B.C. Available at http://www.robertsbankterminal2.com/wp-content/uploads/DP3-Pre-Operations-EAC-Compliance-Report-Appendix-F.pdf.

British Columbia Marine and Pile Driving Contractors Association (B.C. MPDCA). 2003. Best management practices for pile driving and related operations. B.C. Marine and Pile Driving Contractors Association. Available at https://buyandsell.gc.ca/cds/public/2013/07/26/ae944767124a8ee01e9791edf912e185/bc_marinepilingcontractorspile_driving_bmp.pdf.

Dickerson, C., K. J. Reine, and D. G. Clarke. 2001. Characterization of underwater sounds produced by bucket dredging operations. DOER Technical Notes Collection (ERDC TN-DOER-E14), U.S. Army Engineer Research and Development Center, Vicksburg, MS. Available at http://el.erdc.usace.army.mil/elpubs/pdf/doere14.pdf.

Fisheries and Oceans Canada (DFO). 2013. Environmental Watch Reports for Summer 2013. Available at: http://www.pac.dfo-mpo.gc.ca/science/habitat/frw-rfo/reports-rapports/archives-eng.html.

Fisheries Hydroacoustic Working Group (FHWG). 2008. Agreement in principle for interim criteria for injury to fish from pile driving activities. Prepared for FHWG Agreement in Principle Technical/Policy Meeting, June 11, 2008, Vancouver, WA. Available at http://www.dot.ca.gov/hq/env/bio/files/fhwgcriteria_agree.pdf.

Funk, D., D. Hannay, D. Ireland, R. Rodrigues, and W. Koski. 2008. Marine mammal monitoring and mitigation during open water seismic exploration by Shell Offshore Inc. in the Chukchi and Beaufort Seas, July-November 2007: 90-day report. LGL Report P969-1, Prepared by LGL Alaska Research Associates Inc., LGL Ltd., and JASCO Research Ltd. for Shell Offshore Inc., National Marine Fisheries Service (U.S.), and U.S. Fish and Wildlife Service.

Hamilton, E. L. 1980. Geoacoustic modeling of the sea floor. Journal of the Acoustical Society of America 68:1313–1340.

Hammer & Steel, Inc. 2014. Bearing Capacity Chart - Delmag Diesel Pile Hammers (Delmag D100-13 Single Acting Diesel Pile Hammer). Available at http://www.hammersteel.com/delmag-d100.html.

Hannay, D. E., J. Delarue, X. Mouy, B. S. Martin, D. Leary, J. N. Oswald, and J. Vallarta. 2013. Marine mammal acoustic detections in the northeastern Chukchi Sea, September 2007-July 2011. Continental Shelf Research 67:127–146.

Ireland, D. S., R. Rodrigues, D. Funk, W. Koski, and D. Hannay. 2009. Marine mammal monitoring and mitigation during open water seismic exploration by Shell Offshore Inc. in the Chukchi and Beaufort Seas, July-October 2008: 90-day report. LGL Report P1049-1.

MacGillivray, A. O. 2013. A model for underwater sound levels generated by marine impact pile driving. 166th Meeting of the Acoustical Society of America 134:22.

Marczak.W. 1997. Water as a standard in the measurements of speed of sound in liquids J. Acoust. Soc. Am. 102(5) pp 2776-2779. Available at: https://www.researchgate.net/publication/243521223_Water_as_standard_in_the_measurements_of_speed_of_sound_in_liquids.

Miles, P. R., C. I. Malme, and W. J. Richardson. 1987. Prediction of drilling site-specific interaction of industrial acoustic stimuli and endangered whales in the Alaskan Beaufort Sea. OCS Study, MMS 87-0084. BBN Report No. 6509, USDOI. MMS, Alaska OCS Region, Anchorage, AK.

O'Neill, C., D. Leary, and A. McCrodan. 2010. Sound source verification. Pages 1–34 in M. K. Blees, K. G. Hartin, D. S. Ireland, and D. Hannay, editors. Marine mammal monitoring and mitigation during open water seismic exploration by Statoil USA E&P Inc. in the Chukchi Sea, August-October 2010: 90-day report. LGL Report P1119, Prepared by LGL Alaska Research Associates Inc., LGL Ltd., and JASCO Applied Sciences Ltd. for Statoil USA E&P Inc., National Marine Fisheries Service (U.S.), and U.S. Fish and Wildlife Service.

Pile Dynamics Inc. 2010. GRLWEAP. Available at http://www.pile.com/pdi/products/grlweap/.

Puar, S. S. 1996. Seismic response to the George Massey Tunnel. M.Sc. Thesis, University of British Columbia, Vancouver, B.C.

Robinson, S. P., P. D. Theobald, G. Hayman, L-S. Wang, P. A. Lepper, V. F. Humphrey, and S. Mumford. 2011. Measurement of underwater noise arising from marine aggregate dredging operations. MEPF Ref No. 09/P108, Marine Aggregate Levy Sustainability Fund (MALSF). Available at https://dspace.lboro.ac.uk/dspace-jspui/handle/2134/9610.

Southall, B. L., A. E. Bowles, W. T. Ellison, J. J. Finneran, R. L. Gentry, C. R. Green Jr., D. Kastak, D. R. Ketten, J. H. Miller, P. E. Nachtigall, W. J. Richardson, J. A. Thomas, and P. L. Tyack. 2007. Marine mammal noise exposure criteria: initial scientific recommendations. J. A. Thomas and K. Dudzinski, editors. Aquatic Mammals 33:411–509.

Warner, G., C. Erbe, and D. Hannay. 2010. Underwater sound measurements. Pages 1–54 *in* C. M. Reiser, D. W. Funk, R. Rodrigues, and D. Hannay, editors. Marine mammal monitoring and mitigation during open water shallow hazards and site clearance surveys by Shell Offshore Inc. in the Alaskan Chukchi Sea, July-October 2009: 90-day report. LGL Report P1112-1, Prepared by LGL Alaska Research Associates Inc., and JASCO Applied Sciences for Shell Offshore Inc., National Marine Fisheries Service (U.S.), and U.S. Fish and Wildlife Service.

Warner, G., C. O'Neill, A. McCrodan, H. Frouin-Mouy, J. Izett, and A. MacGillivray. 2013. Underwater acoustic measurements in Haro Strait and Strait of Georgia: transmission loss, vessel source levels, and ambient measurements. Version 2.0 DRAFT Technical Report, Document 00659, Prepared by JASCO Applied Sciences for Hemmera Envirochem Inc.

Zhang, Y., and C. Tindle. 1995. Improved equivalent fluid approximations for a low shear speed ocean bottom. Journal of the Acoustical Society of America 98:3391–3396.

Zykov, M., A. MacGillivray, M. Austin, O. McHugh, M. Fraker, and B. Wheeler. 2007. Source level study of the dredge Columbia and killer whale acoustics impact report update. Technical Report, Prepared by JASCO Research and Jacques Whitford AXYS for Vancouver Port Authority.